Medical Bio EX Proposal Report

Proposal number:

2009A1878

Title of experiment:

Dynamic synchrotron x-ray detection of individual pollutant particle behaviour after deposition onto live airways

Name and affiliation of the project leader:

Dr David Parsons, Women's and Children's Hospital, North Adelaide, South Australia

Beamline used:

BL20XU Downstream

Research purpose and background

In our industrialised society, air pollution is a significant environmental and health concern. Man-made airborne pollutants from a wide variety of sources are suspended in the air in liquid, gaseous or solid forms. We have previously reported a new technique to image samples of solid particulates such as quarry dust, fibreglass, asbestos fibres, and lead in mouse nasal airways [1]. These particulates have the potential to produce deleterious acute or delayed health effects that can impact on asthma, cystic fibrosis (CF), bronchitis, emphysema, lung and heart disease, and respiratory allergies.

Mucociliary transit (MCT), and therefore the effectiveness by which the airways clear any inhaled pollutant particles, is a clear airway health diagnostic indicator. In attempting to determine the effectiveness of genetic [2, 3] and other potential therapeutics for CF airway disease we have developed MCT monitoring methods that can be used *in-vivo* in mice. Existing methods for quantifying bulk particle clearance in airways [4] are unable to non-invasively detect and track the motion of individual pollutant particles in real time and with high resolution. Direct visualisation of the behaviour of deposited particles in animal model airways is expected to improve our understanding of airway surface function and suggest novel methods for prevention or treatment of respiratory disease.

In 2008B we demonstrated the ability to locate, track and quantify the motion of common inhaled particles in the nasal airways of live mice using phase contrast X-ray imaging (PCXI). The lung airways remain the relevant target organ, so the aim of the 2009A study was to extend our previous work to non-invasively examine particulate deposition and MCT in the lung airways of live mice.

Experimental/analytical method

The PCXI experiment was performed in the downstream BL20XU hutch. The imaging and experimental setups are described in three publications [1, 5, 6]. The experiment consisted of an *in-vitro* study to confirm the visibility of a range of biologically-relevant particulates, a pilot *ex-vivo* study to examine the visibility of the particulates in an excised mouse trachea, and an *in-vivo* study to examine the behaviour of the particles after deposition onto live mouse airways.

The same potentially respirable pollutant particles visible in the 2008B study were examined suspended in saline carrier fluid to verify their visibility using PCXI. Chrysotile (white asbestos) and fibreglass from a commercial pipe insulation were separately ground under water to produce fibres suited for examination. Galena (lead ore) and dolomite quarry dust were also tested. Raw samples were prepared

in physiological saline at concentrations of 0.1% w/v and 1% w/v, and 15µl samples were pipetted inside small steel washers placed on the exposed adhesive surface of Kapton tape. The particles and liquid were then sealed in place inside the washers using a second piece of tape and the samples were mounted on a controllable X-Y stage in the hutch for imaging.

A pilot *ex-vivo* experiment was performed using one HOS:HR-1 mouse. The mouse was humanely killed via Nembutal overdose and the trachea was surgically excised before being placed into a study chamber where it was held between two 20Ga i.v. catheters. Thin films of Kapton sealed the front and rear of the chamber to minimise specimen dehydration during the experiment. The chamber was mounted on the x-y-rotation stage in the imaging hutch such that the X-ray beam passed laterally through the excised trachea; the same orientation used in the *in-vivo* studies. Images were captured at baseline and after delivery of 15 µl samples of the particulates suspended in saline. The stage was also translated in the x-direction to allow the full length of the excised trachea to be imaged using a number of exposures.

In-vivo experiments were performed using 15 HOS:HR-1 mice. Groups of three mice were exposed to each of the five particulates. Mice were anaesthetised with Nembutal and then intubated using a 20Ga i.v. catheter as an endotracheal (ET) tube. Mice were secured to a polyethylene imaging board, with dorsal incisors hooked over a stainless-steel wire loop and the limbs, shoulders and torso were taped to minimise respiratory movements. The imaging board was mounted on the x-y-rotation stage in the hutch such that the X-ray beam passed laterally through the mouse trachea, at approximately three cartilage rings below the tip of the ET tube. The ET tube was connected to a flexiVent small animal ventilator, and anaesthesia was maintained using a humidified isoflurane O_2 mixture. The ventilatory profile was configured with an end-inspiratory pause to allow unblurred image capture.

Image capture was triggered by the ventilator once every 14 breaths (10.5 sec). After 3.5 minutes of baseline collection (20 images), a 15 µl sample of the particulate suspended in saline was manually delivered via the ET tube in a single bolus delivered over 10 seconds. Image acquisition was resumed at the same rate for a further 42 minutes (~240 images), creating a dataset consisting of 260 images.

Research results

The *in-vitro* PCXI visibility of the pollutant particles in saline was similar to what we previously reported for samples in distilled water [1]. Based on our *in-vitro* observations a concentration of 1% w/v was selected for both *ex-vivo* and *in-vivo* studies, to ensure sufficient particulates were present in a 15 µl sample to potentially be visible when deposited into the mouse trachea.

Prior to use in live mice the *ex-vivo* visibility of the particulates was also verified in a segment of excised mouse trachea. All particulates could be easily detected and had similar appearances to the *in-vitro* study (all particulates are visible in Figure 1a). Although all particulates were detectable, the smaller and less visible quarry dust particles were harder to detect than fibreglass, galena and the hollow glass beads. In addition, only one bundle of asbestos fibres was visible in the trachea in contrast to the other particulates, of which many individual particles could be detected. Despite using an enclosed chamber we did find that the excised trachea tended to rapidly and visibly dehydrate, and thus we did not attempt to use this system to analyse MCT behaviour.

A 15 µl dose volume provided sufficient visible fluid and particulates to be monitored in the trachea and induced no noticeable change in respiratory effort or frequency. We noted that for the first 30 minutes of the experiment image quality was excellent, due largely to the respiratory-gating. After approximately 30 minutes most mice displayed large irregular respiratory excursions initially every ~10 breaths, increasing in frequency and magnitude as the experiment continued. Mice remained deeply anaesthetised, but these movements eventually degraded the quality of the images because the

end-inspiratory breath holds became ineffective. Independently increasing the level of anaesthesia and tidal volume had no effect. We trialed imaging one mouse in a supine position which largely eliminated the irregular respiratory movements suggesting that the head-high mounting was a likely cause of the respiratory instability we observed.

Fibreglass, galena, quarry dust and the hollow silver coated glass beads could be detected *in-vivo* in some animals, although with different degrees of visibility and with varying levels of difficulty. We did not positively identify asbestos fibres in any of the image sequences. Of the particulates that we could detect with PCXI, galena was the simplest and quarry dust the most difficult. Fibreglass and the hollow silver coated glass beads were intermediate.

Although there was little bulk saline present during imaging, the liquid layer present on the airway surface was consistently thicker on the dorsal side of the trachea. Independent of the particle type and size, the majority of particle deposition and particle motion also occurred on the dorsal side of the trachea. In those animals in which particulates were detected they were visible throughout the entire imaging period. However, most particle motion in the trachea occurred within the first few minutes of imaging, with almost all particles eventually lodging. Almost all galena particulates appeared to be motionless from the initiation of imaging (~1 minute after dose delivery), but in comparison some glass beads continued moving for almost the entire imaging period before eventually lodging after 30+ minutes. The motion and lodging of quarry dust and fibreglass were between these two extremes. In general, small particles continued their motion for longer than large particles; the latter were observed to lodge quickly on the airway surface.

Figure 2 shows a quarry dust particle moving over a period of 2.1 minutes. The MCT rate of this particle (and many others) was not uniform, and varied between zero and ~0.5 mm/min. Figure 3 shows a single image of stationary fibreglass fibres present in the trachea. Interestingly, in this animal a small number of fibres were present on the ventral surface, although most collected along the dorsal surface. Galena particles did not move substantially over the imaging period, but were the easiest particulate to detect *in-vivo*. Large clusters of galena approximately 60 μm long were present in two mice, and in one animal the galena cluster moved between two points in the airway rather than staying stationary. This was contradictory to the behaviour of most other large particles which, as previously noted, tended to lodge quickly. Figure 4 shows the behaviour of this large cluster, with both the transit motion and clump orientation noted, showing rotation during MCT movement. Figure 5 shows the motion of multiple glass beads along the dorsal tracheal surface and like galena their particle motion was not uniform; beads could move in different directions, and at different rates. The MCT rate of the marked particles varied between -0.02 mm/min (down the trachea) and 0.37 mm/min (toward the larynx). In the same animal we measured smaller glass beads moving at more than twice this rate (up to 0.75 mm/min) however they cannot be seen on these static images.

In summary, this project examined how different types of particles moved along the airways; and established the potential of this new non-invasive imaging method to assist in research into the initiation of childhood and other respiratory diseases that are related to particulate inhalations.

Current and future issues/challenges

The aerodynamic diameter of inhaled particulates must be less than 10 μm to be inhaled into the lung of humans. An improvement in the minimum size detectable under PCXI will be important for ensuring biological relevance in future instillation or inhalation studies.

We also suspect that changing from head-high to supine imaging will reduce loading on the diaphragm that likely causes muscle fibre shortening, ventilatory loading and potential hypoxaemia and hyercapnia. Venous return problems when vertical can also reduce cardiac output and potentially

metabolism. We expect that mice will not exhibit the large unpredictable respiratory excursions that currently cause image blurring and limit usable imaging time to <30 minutes. Supine imaging will impose more physiologically realistic gravitational effects on particle motion, assisting us to quantify true post-deposition MCT behaviour.

In these first studies little effort was made to limit radiation dose, which was too intense to consider animal recovery and repeated imaging. The current rapid development of synchrotron and imaging technology suggest there will continue to be improvements in CCD sensor technology, and analytical techniques such as motion-detection and particle tracking. Combined, they should lead to improved image resolution and higher light sensitivity, allowing smaller — and therefore more physiologically relevant — particulates to be detected and tracked.

References

[1] M. Donnelley, K. Morgan, A. Fouras, W. Skinner, K. Uesugi, N. Yagi, K. Siu, and D. Parsons, "Real-time non-invasive detection of inhalable particulates delivered into live mouse airways," *Journal of Synchrotron Radiation,* vol. 16, pp. 553-561, 2009.

[2] M. Limberis, D. S. Anson, M. Fuller, and D. W. Parsons, "Recovery of airway cystic fibrosis transmembrane conductance regulator function in mice with cystic fibrosis after single-dose lentivirus-mediated gene transfer (vol 13, pg 1961, 2002)," *Human Gene Therapy,* vol. 13, pp. 2112-2112, Nov 2002.

[3] A. Stocker, K. Kremer, R. Koldej, D. Miller, D. Anson, and D. Parsons, "Single-dose lentiviral gene transfer for lifetime airway gene expression," *The Journal of Gene Medicine,* 2009.

[4] B. R. Grubb, J. H. Jones, and R. C. Boucher, "Mucociliary transport determined by in vivo microdialysis in the airways of normal and CF mice," *Am J Physiol Lung Cell Mol Physiol,* vol. 286, pp. L588-595, March 1, 2004 2004.

[5] D. W. Parsons, K. Morgan, M. Donnelley, A. Fouras, J. Crosbie, I. Williams, R. C. Boucher, K. Uesugi, N. Yagi, and K. K. W. Siu, "High-resolution visualization of airspace structures in intact mice via synchrotron phase-contrast X-ray imaging (PCXI)," *Journal of Anatomy,* vol. 213, pp. 217-227, Aug 2008.

[6] M. Donnelley, K. Morgan, A. Fouras, W. Skinner, K. Uesugi, N. Yagi, K. Siu, and D. Parsons, "A new approach to examining individual particle deposition and clearance from live mouse lung airways," *To be submitted Aug,* 2009.

[7] B. R. Grubb and R. C. Boucher, "Pathophysiology of gene-targeted mouse models for cystic fibrosis," *Physiological Reviews,* vol. 79, pp. S193-214, 1999.

Status of publication and patent

From this experiment we are preparing to publish article number 6 in the references above.

Keywords and annotations

particles; pollution; airway surface; lung; trachea; mucociliary transit; non-invasive; synchrotron radiation; X-ray imaging; X-ray phase-contrast; radiography; mouse;

Figs

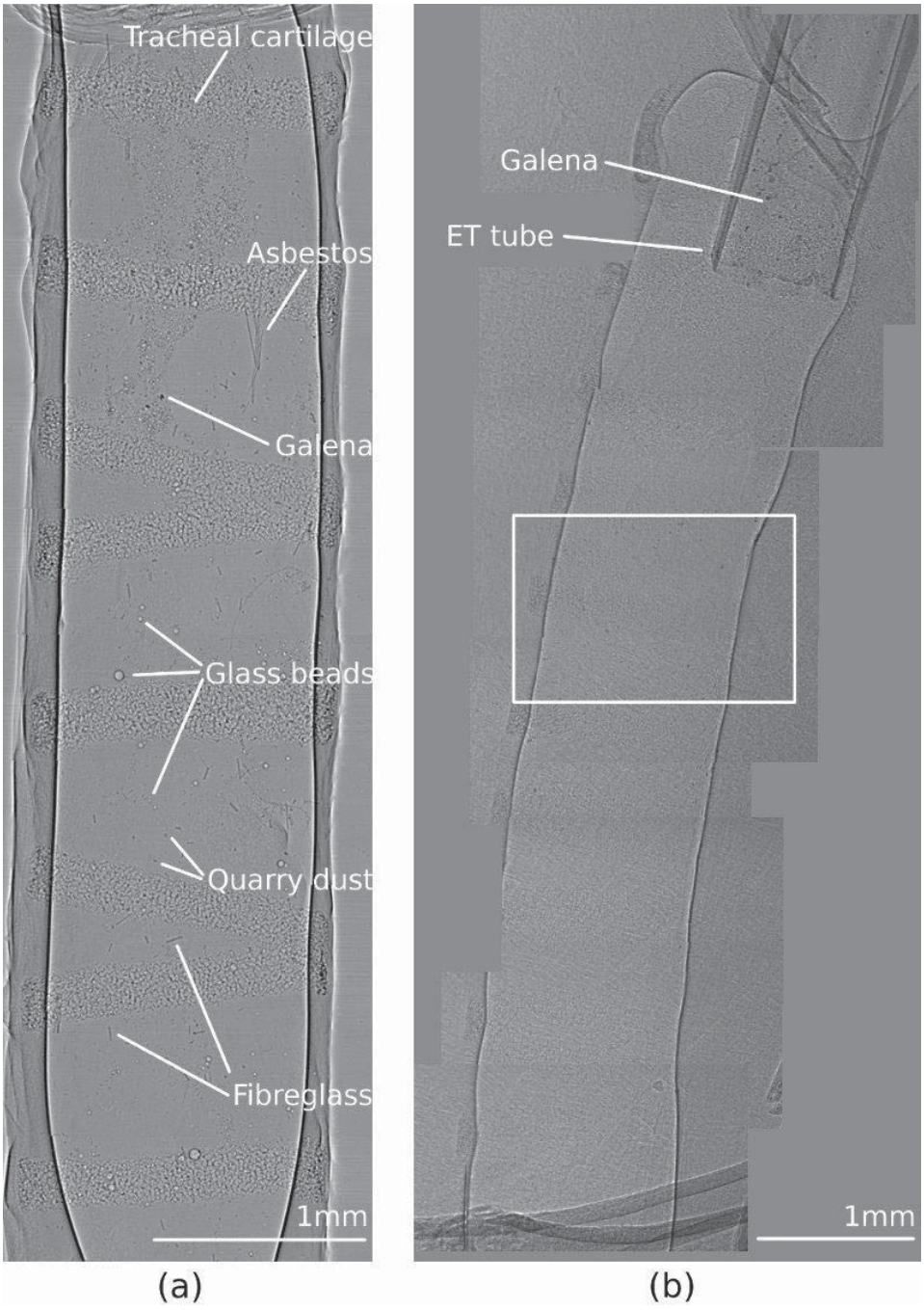

Figure 1 (a) A montage of 9 individual PCXI images from the pilot *ex-vivo* experiment that examined an excised mouse trachea. The images were taken after all 5 particulates had been delivered within individual 15 μl boluses. All 5 particle types are clearly visible and marked. (b) An *in-vivo* montage of 15 individual PCXI images with the ET tube uppermost in the trachea. The ET tube opening is approximately 2 cartilage rings from the top, and the standard imaging location, usually 3 rings below the bottom of the ET tube, is marked with a white rectangle. Dark particles of galena are apparent within the ET tube as well as at the imaging site in the trachea. Image alignment is poor at some montage frame edges due to respiratory movements that occurred between image captures.

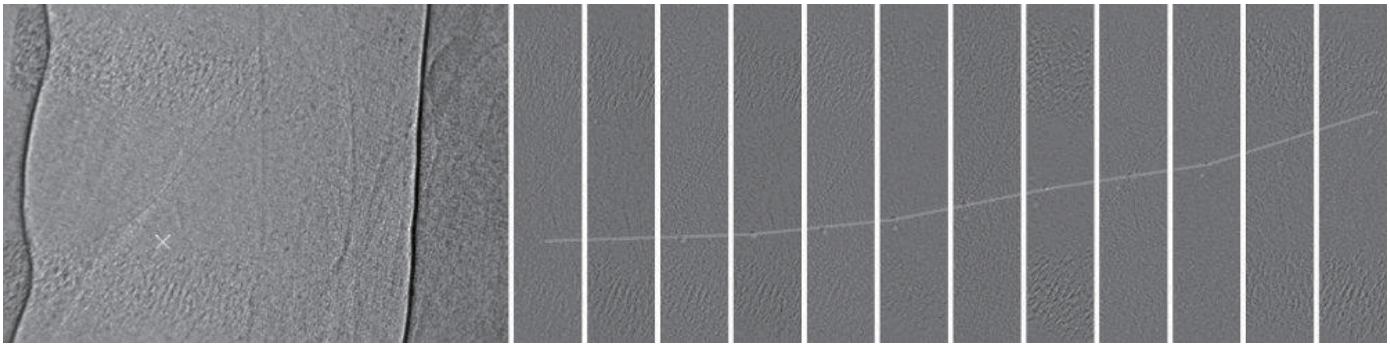

Figure 2 *In-vivo* imaging of quarry dust in a live mouse trachea. The image on the left (1.8 x 1.2 mm) was captured approximately 1.75 minutes after imaging was started, and the location of a quarry dust particle is marked with an X. The sequence of image strips to the right were created by cropping complete image frames to show the same region in subsequent motion-detected frames, captured 10.5 seconds apart (i.e. 2.1 minutes total). The motion of the dust particle is tracked by the grey line, and demonstrates variability in the rate of particle transit for even a single particle. Other particles were also visible when viewed dynamically, but cannot be seen on these static images.

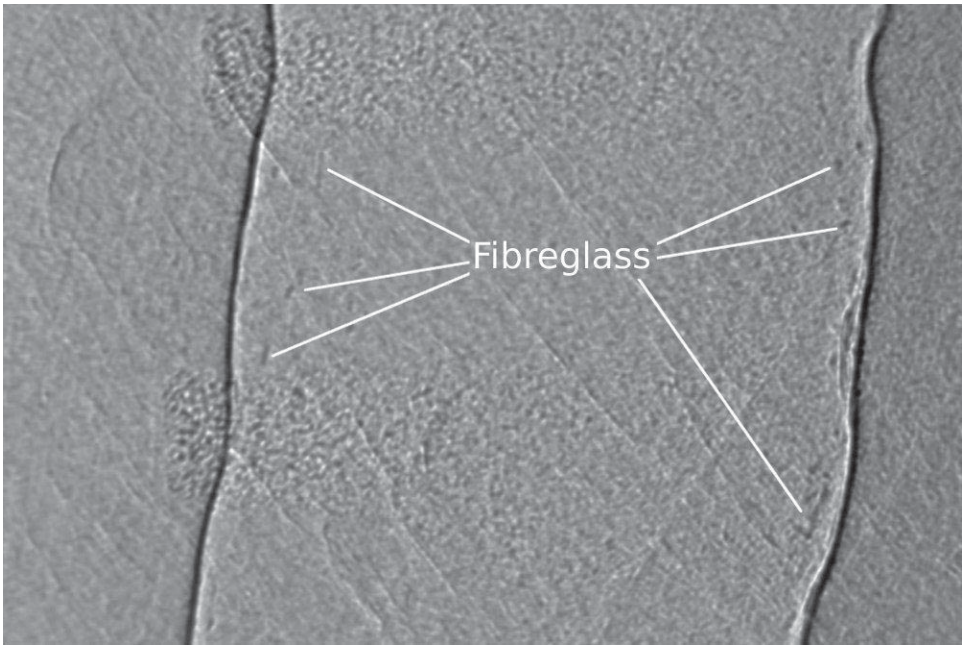

Figure 3 *In-vivo* imaging of fibreglass in a live mouse trachea. This is the first image (1.8 x 1.2 mm) captured after imaging began, and although the fibres were visible in the trachea, they did not move throughout the imaging period. Although most fibres were located on the dorsal tracheal surface (the right hand side of the image) in this animal a small number were also visible on the ventral surface.

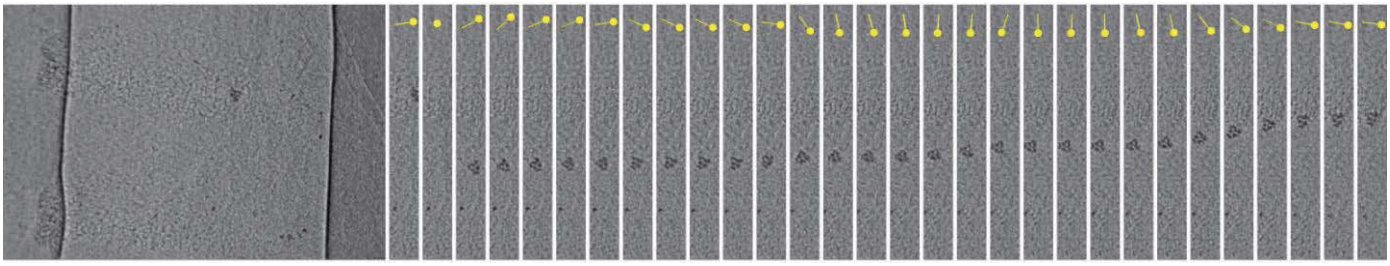

Figure 4 *In-vivo* imaging of galena in a live mouse trachea. The image on the left (1.8 x 1.2 mm) is the first image captured after imaging began, and shows a large clump of lead particles, as well as smaller individual particles spread throughout the trachea. The strips on the right are from the first 30 frames, each captured 10.5 seconds apart (i.e. 5.25 minutes total), and show the motion of the lead clump. The indicator at the top of each strip shows the relative rotation of the clump. Note that between the 1st and 3rd strips the clump movement was briefly retrograde. The majority of the other individual galena particles are located toward the dorsal tracheal wall (the right-hand side of the image).

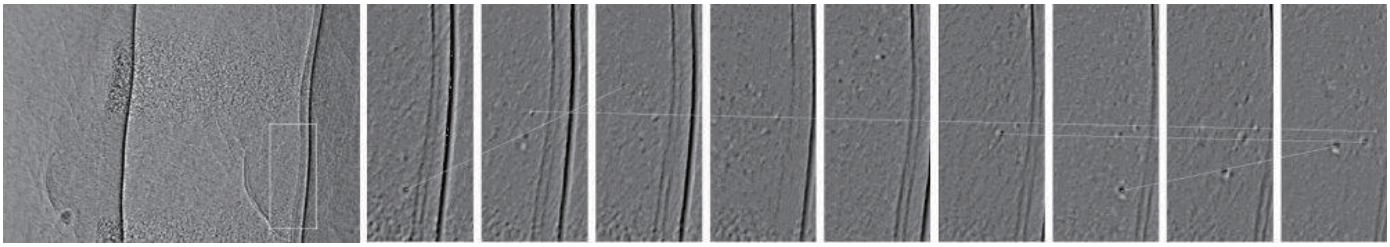

Figure 5 *In-vivo* imaging of silver coated hollow glass beads in a live mouse trachea. The image on the left (1.8 x 1.2 mm) was captured approximately 2 minutes after imaging was started. The strips on the right are motion detected frames 42 seconds apart (i.e. 5.6 minutes total) from within the marked white rectangle. The motion of 4 separate particles is marked; two are moving up the trachea at different speeds, and two are moving more slowly down the trachea. A large number of smaller particles moved faster than these, but are not clear on these static images. The majority of the glass bead particle transit was located toward the dorsal tracheal wall (the right-hand side of this image).